Information Content of GMI Radiances in a Dual-Frequency Radar Profiling Algorithm

S. Joseph Munchak[1,2], Benjamin Johnson[1,3], Mircea Grecu[1,4], and William S. Olson[1,3]

1: NASA Goddard Space Flight Center; 2: University of Maryland/ESSIC; 3: University of Maryland Baltimore County/JCET, 4: Morgan State University

Motivation

The combination of the DPR and GMI instruments on the GPM core satellite will offer an unprecedented array of observations with which to constrain retrievals of precipitation. However, optimally combining the data from these two instruments requires knowledge of the sensitivity of the measurements to properties of precipitating and non-precipitating atmospheric constituents and the surface. This work seeks to identify those properties which are well constrained by the observations and those that are not (but nevertheless impact the retrieved precipitation parameters), and should therefore be obtained from ancillary sources or in-situ measurements as appropriate.

Summary of Parameters

The retrieval paradigm being used here is a dual-frequency radar algorithm that can retrieve two parameters of the DSD (N_0 and D_m) at each range gate, given assumptions of the third parameter (μ), along with cloud water and water vapor profiles and hydrometeor phase information. These assumptions, if incorrect, can lead to errors in the retrieved parameters both directly and indirectly. An example of a direct effect is that if the assumption regarding μ is incorrect, the values of D_m and R will be incorrect for a given reflectivity pair. An indirect effect, such as an incorrect cloud water profile assumption, leads to an error in the attenuation estimate which is used to correct the reflectivities before they are used to retrieve the DSD parameters. The following table lists some of these assumptions and their impact upon the GPM observations.

Algorithm Assumption	Impact on:								
	Z14	Z35	T10	T19	T23	T37	T89	T166	T183
DSD (rain)	D	D	D	D	D	D	N	N	N
PSD (ice)	D	D	N	N	N	D	D	D	D
Cloud Water	I	I	D	D	D	D	D	D	D
Water vapor	N	I	N	N	D	N	D	D	D
Ice Scattering Model	D	D	N	N	N	D	D	D	D
Surface Emissivity	N	N	D	D	D	D	D	D	N

Table 1: Partial list of dual-frequency radar algorithm assumptions and effect upon radar (Z) and radiometer (T) observations (D=direct, I=indirect, N=negligible).

Sensitivity Tests

In the two figures below, the sensitivity of retrievals to changes in a selection of the assumptions listed in Table 1 are illustrated. The reference retrieval uses a "fluffy sphere" Mie snow particle model, shape parameter μ=3, and a low cloud water profile. Deviations from these assumptions take the following forms:

- Replace μ=3 with σ_m-D_m relationship derived from disdrometer data
- Replace Mie sphere with Discrete Dipole Approximation of a 20-flake aggregate
- Replace low cloud water profile with high cloud water profile
- Double surface wind speed from 7 to 15 m/s (only affects Tbs; retrieved profiles not shown)

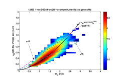
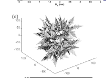
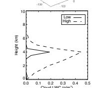

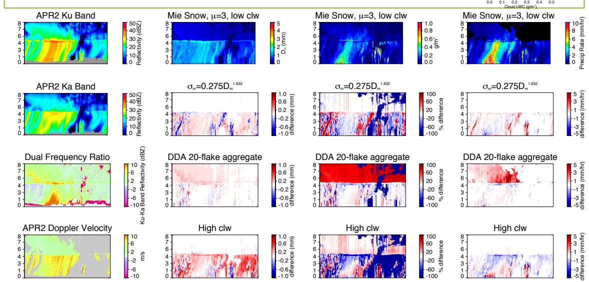

Figure 1: Cross-sections of APR2 measurements (1st column), retrieved D_m (2nd column), LWC (3rd column), and precipitation rate (4th column) under various algorithm assumptions. APR2 are taken from over the Gulf of Mexico on August 17,2010 during the GRIP field experiment and courtesy of Simone Tanelli (JPL).

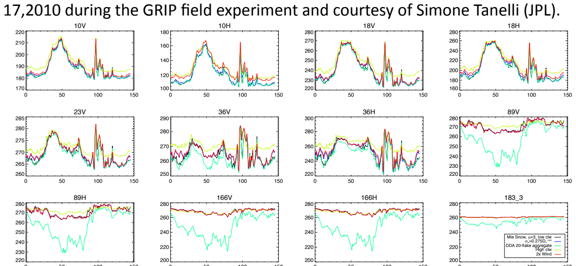

Figure 2: Simulated GMI brightness temperatures corresponding to the four retrieved profiles in Figure 1 plus a fifth profile identical to the first except for a doubling of wind speed (increasing surface emissivity).

Potential Impact on Retrievals

Three archetypal reflectivity profiles were selected to quantify the constraint imposed by GMI radiances on the radar solution space. From each radar profile 3,000 profiles and associated brightness temperatures were generated from random combinations of:

- 40 model-derived cloud water and water vapor profiles
- 6 values of μ (range from 1-6)
- Surface wind speed (0-30 m/s)

For each ensemble member *i*, a subset of ensemble was defined consisting of those profiles where all T_bs were within 3K of *i*'s T_bs. The subset mean and variance were then calculated. The mean subset variance and correlation between the value of the i^{th} profile and its corresponding subset mean are presented in Table 2.

Parameter	Warm Rain			Stratiform Rain			Convective Rain		
	EV	SV	r^2	EV	SV	r^2	EV	SV	r^2
Cloud LWP (kg/m²)	0.44	0.28	0.13	0.40	0.27	0.12	0.51	0.26	0.12
Rain LWP (kg/m²)	0.05	0.02	0.76	0.06	0.02	0.67	0.23	0.11	0.45
TPW (mm)	15.1	13.3	0.08	11.6	13.8	0.00	15.3	13.2	0.01
Sfc wind (m/s)	19.0	4.6	0.92	15.9	5.8	0.92	18.9	14.5	0.44
Sfc R (mm/hr)	1.06	0.54	0.71	0.15	0.08	0.52	5.87	1.28	0.72
Sfc D_0 (mm)	0.15	0.05	0.76	0.06	0.03	0.49	0.16	0.04	0.69

Table 2: GMI information content metrics for various physical parameters (LWP=liquid water path, TPW=total precipitable water) in three sample profiles. EV=ensemble variance, SV=subset variance (lower is better), and r^2 is the percentage of variance explained (higher is better).

Conclusions

- GMI radiances provide weak constraints on cloud water content, although there is some sensitivity to supercooled cloud water which weakens ice scattering signal. This emphasizes the need for *a priori* knowledge of cloud water profiles and their association with other observables (e.g., echo top, rain classification).
- Rain parameters (LWP, R, and D_0) are well-constrained by the T_bs in these simulations. Often this is a result of radiances favoring one solution when dual solutions to the radar profile are present.
- There is essentially no information regarding water vapor *in precipitation* despite the water vapor channels on GMI.
- There is a high sensitivity to surface emissivity in the low-frequency channels except in the heaviest rain. Given the radar constraint on the precipitation profile, this points to an ability to retrieve wind speed in precipitation over water surfaces.